PHILOSOPHICAL TRANSACTIONS OF THE ROYAL SOCIETY A MATHEMATICAL, PHYSICAL & ENGINEERING SCIENCES

Skylark Rocket Observations of Ultraviolet Spectra of $\gamma ^{2}$ Velorum and $\zeta $ Puppis

W. M. Burton, R. G. Evans and W. G. Griffin

Phil. Trans. R. Soc. Lond. A 1975 **279**, 355-369
doi: 10.1098/rsta.1975.0069

Phil. Trans. R. Soc. Lond. A. **279**, 355–369 (1975) [355]
Printed in Great Britain

Skylark rocket observations of ultraviolet spectra of γ^2 Velorum and ζ Puppis

By W. M. Burton, R. G. Evans and W. G. Griffin
Astrophysics Research Division of the Appleton Laboratory,
Culham Laboratory, Abingdon, Oxfordshire

A star-stabilized Skylark rocket was launched from Woomera in June 1973 to record ultraviolet spectra of the bright stars γ^2 Velorum and ζ Puppis. The instrumentation consisted of three Wadsworth-mounted objective grating spectrographs with a combined wavelength range 90–230 nm. Stellar spectra were recorded on Kodak 101-01 photographic film, the in-flight spectral resolution being approximately 30 pm. Two exposures were obtained on each of the target stars. The γ^2 Vel spectrum observations extend from 92 to 230 nm and the ζ Pup spectrum from 100 to 230 nm. Analysis of the spectra provides information about the composition and properties of the interstellar gas in the line of sight. The observations also provide useful data on the stellar atmospheres. P Cygni line profiles are observed in the spectra of both stars indicating that high velocity material is being ejected.

Introduction

Far ultraviolet spectra of the bright southern hemisphere stars γ^2 Velorum and ζ Puppis were recorded on 15 June 1974 using spectrographic instrumentation carried on a star-stabilized Skylark rocket. The two-stage rocket vehicle was launched from Woomera, South Australia, and reached an altitude of 227 km, providing about 3 min of stabilized observation time above 120 km before the payload was recovered by parachute. The instrumentation consisted of a package of three Wadsworth-mounted objective grating spectrographs, each of which recorded spectra on Kodak 101-01 photographic film.

During the stabilized period of the rocket flight two exposures (78 and 24 s) were obtained for γ^2 Vel and two exposures (40 and 22 s) for ζ Pup. The observations have a spectral resolution $d\lambda \simeq 30$ pm and cover the wavelength range 92–230 nm for γ^2 Vel and 100–230 nm for ζ Pup. A description of the observations and a preliminary analysis has been given by Burton *et al.* (1973) and a detailed analysis of the interstellar line spectrum will be published elsewhere (Burton, Evans & Griffin 1974). The present paper gives a summary of the main conclusions of the interstellar spectrum analysis, together with a discussion of some stellar spectral features and their interpretation.

The interstellar spectrum

The spectral resolution of the present observations is adequate to distinguish stellar absorption features, which are generally much wider than the instrument resolution (*ca.* 30 pm), from the interstellar lines which are intrinsically narrow and are therefore recorded with the limiting instrumental resolution. This resolution corresponds to about 75 km s^{-1} and is consequently insufficient to resolve individual interstellar cloud velocities, but the measured equivalent widths provide useful information about the total column densities of ions in the line of sight through the interstellar medium. Table 1 gives a list of the interstellar lines observed in the spectra of γ^2 Vel and ζ Pup, together with the measured equivalent widths. The column

density of absorbing interstellar material can be calculated from the equivalent widths of the absorption lines by the curve of growth method. The calculation of the curve of growth requires a detailed knowledge of the line of sight velocity distribution of the absorbing material which is obtainable from very high resolution optical spectra. Unfortunately no such data has been published for γ^2 Vel and ζ Pup.

TABLE 1. INTERSTELLAR LINE EQUIVALENT WIDTHS

λ/nm	ion	$W(\gamma^2$ Vel)/pm	$W(\zeta$ Pup)/pm	$W(\gamma^2$ Vel)/$W(\zeta$ Pup)
92.62	HLη	11.3	—	—
93.07	HLζ	15.6	—	—
94.97	HLδ	15.3	—	—
98.88	O I	15.0	—	—
98.98	N III, Si II	12.0	—	—
102.57	HLβ	present	present	—
103.63	C II	11.4	18.0	0.63
103.70	C II	7.8	11.0	0.71
103.92	O I	9.7	16.5	0.59
104.82	A I	6.0	11.0	0.55
108.40	N II	6.5	7.0	0.93
108.46	N II	5.5	8.0	0.68
108.57	N II	4.0	7.0	0.57
119.04	Si II, S III	14.0	17.3	0.81
119.33	Si II	12.3	14.0	0.88
119.95	N I	10.0	14.2	0.7
120.02	N I	—	10.6	—
120.07	N I	—	10.6	—
120.65	Si III	16.8	26.0	0.65
121.57	HLα	490	600	—
125.03	S II	—	8.3	—
125.38	S II	7.8	9.5	0.82
125.95	S II	7.0	10.7	0.65
126.04	Si II	15.0	19.4	0.77
130.22	O I	13.5	15.1	0.89
130.44	Si II	10.0	13.5	0.74
133.45	C II	12.0	16.0	0.75
133.57	C II	10.0	15.0	0.67
152.67	Si II	10.0	16.7	0.60
167.08	Al II	11.0	18.0	0.61
185.47	Al III	8.0	9.5	0.84
186.28	Al III	7.0	5.9	1.2
187.31	Si I	4.0	3.0	1.33
187.58	Si I	4.0	2.0	2.0
188.10	Si I	6.0	—	—

It is, however, possible to calculate the column density of atomic hydrogen from the observed Lyman α absorption line (λ = 121.6 nm) without any knowledge of the line of sight velocity distribution. The interstellar absorption in HLα is so strong that the absorption line is formed mainly in the radiation damped wings and the equivalent width is then nearly independent of the velocity distribution. Figure 1 shows a densitometer tracing of the HLα line in the spectrum of ζ Pup. The H I column density has been obtained by fitting theoretical absorption

line profiles to the observed spectra, a procedure used by Smith (1970) and others. The theoretical profile is given by $I(\lambda) = I_0 \exp(-\tau_\lambda)$ and in the wings of the line, where radiation damping predominates, the optical depth is given by $\tau_\lambda = 9.25 \times 10^{-26} (\lambda - \lambda_0)^{-2} N_H$, with λ and λ_0 in nm and N_H in atom m^{-2}. The line profiles obtained by this method for various column densities N_H were compared with the observed line profiles obtained from the densitometer traces and the characteristic curve of the photographic film. Both exposures on each star were used to obtain the following column densities of neutral hydrogen:

γ^2 Vel: $N_H = (4.5 \pm 1.5) \times 10^{23}$ atom m^{-2}, ζ Pup: $N_H = (6.7 \pm 1.0) \times 10^{23}$ atom m^{-2}.

These values are consistent with previously reported measurements of N_H for γ^2 Vel of $(3.2 \pm 1.7) \times 10^{23}$ (Carruthers 1968) and for ζ Pup of $(5.9 \pm 1.8) \times 10^{23}$ (Carruthers 1968), $(4.8 \pm 1.7) \times 10^{23}$(Morton, Jenkins & Brooks 1969) and $(7.6 \pm 2.5) \times 10^{23}$ (Smith 1970), all in units of atom m^{-2}.

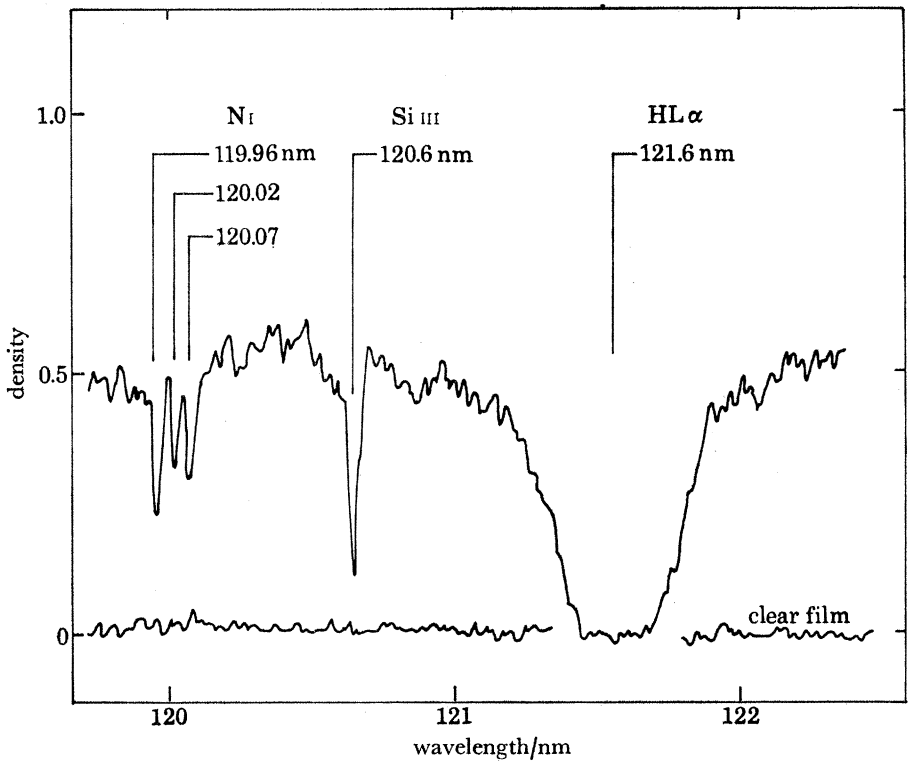

FIGURE 1. Densitometer tracing of the ζ Pup spectrum in the wavelength range 119.5–122.5 nm showing lines of N I ($\lambda \approx 120.0$ nm), Si III ($\lambda = 120.6$ nm) and HLα ($\lambda = 121.6$ nm).

To determine the average line of sight density of atomic hydrogen in the interstellar medium from the measured H I column density, it is necessary to estimate the path length through neutral hydrogen. The two stars γ^2 Vel and ζ Pup are located at a distance of about 450 pc from the Sun, near to the centre of the large Gum Nebula H II region which is shown schematically in figure 2. Brandt, Stecher, Crawford & Maran (1971) have suggested that the Gum Nebula is the 'fossil Strömgren sphere' associated with the Vela X supernova remnant, but other interpretations have also been proposed (e.g. by Bok 1971). Both γ^2 Vel and ζ Pup are probably surrounded by Strömgren sphere H II regions with diameters of about 60 pc, leaving a distance of *ca.* 420 pc through the true interstellar medium. The H I densities deduced from this path

length are 3.6×10^4 m^{-3} to γ^2 Vel and 5.3×10^4 m^{-3} to ζ Pup, both rather low compared with the value of $3.5 \pm 1 \times 10^5$ m^{-3} recently estimated by Macchetto & Panagia (1973) for the atomic hydrogen density in the intercloud medium. In considering the earlier measurements of the H I density to γ^2 Vel and ζ Pup, Brandt *et al.* (1971) suggest that the Gum H II region extends to within about 100 pc of the Sun, in which case the measured H I column densities refer to a path length of only 100 pc giving an average atomic hydrogen density of about 2×10^5 m^{-3} in the local interstellar gas.

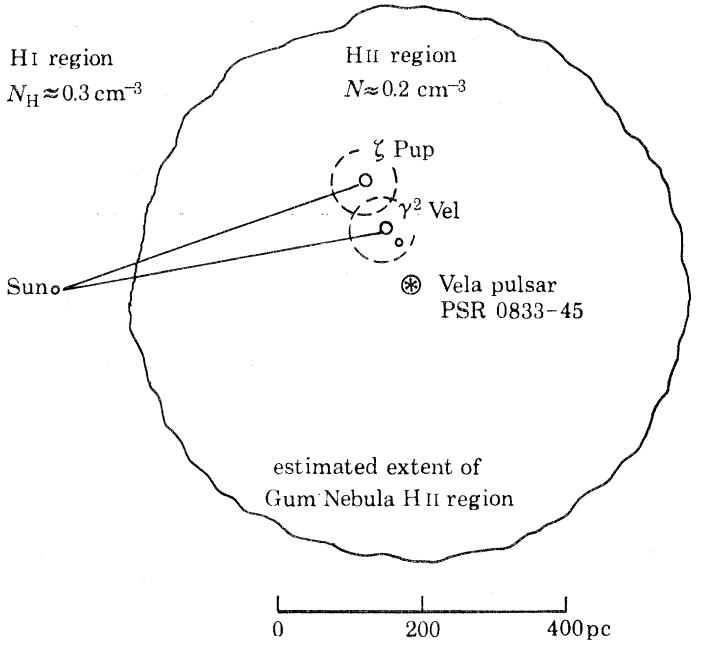

FIGURE 2. Schematic view of the Gum Nebula H II region according to the model of Brandt *et al.* (1971).

In order to calculate the column densities of the other observed interstellar ions both the absorption oscillator strengths and the line of sight velocity distribution of the absorbing material are required. In the absence of high dispersion optical measurements of the line of sight velocity distribution of absorbing material, it is assumed that these velocities are distributed according to a Gaussian distribution with a velocity dispersion $b\sqrt{2}$ km s^{-1}. Curves of growth have been used to estimate the value of b by measuring the strengths of different absorption lines from the ground level and using their relative oscillator strengths to fit the measured points to the curve of growth. Several suitable multiplets occur in the present rocket data including N I (120 nm triplet), Si II (4 lines) and S II (3 lines), the data for ζ Pup being more complete than for γ^2 Vel where the N I and S II lines are blended with stellar features.

The data for ζ Pup give a consistent result only if we adopt a value of $b = 9.4 \pm 0.6$ km s^{-1}. In table 1 the observed equivalent widths show a consistently smaller value for γ^2 Vel than for ζ Pup, the average value of the ratio being 0.74 with a standard deviation of only 0.03. If the γ^2 Vel column densities are calculated using the ζ Pup b value of 9.4 km s^{-1} then the resulting densities are significantly smaller ($\times 0.1$ to $\times 0.3$) than for ζ Pup, but if we use $b = 0.74 \times 9.4$ km s^{-1} $= 7.0$ km s^{-1} for γ^2 Vel, then the column densities for the two stars show reasonable agreement. This interpretation is more consistent with the probable location of the two stars which are thought to be relatively close together (Brandt *et al.* 1971) and the resulting b value is quite consistent with that measured by fitting the γ^2 Vel Si II lines to the curve of growth.

In the case of γ^2 Vel we have obtained an independent derivation of b by making use of the observations of high members of the hydrogen Lyman series. The column density of atomic hydrogen can be determined from the absorption line profile of HLα ($\lambda = 121.6$ nm), the measurement being independent of b because radiation damping predominates in the formation of this strong line. High members of the Lyman series have very small damping constants and may be assumed to lie on the curve of growth calculated for zero damping. Since the atomic hydrogen column density is known from the HLα profile, the optical depth in the high Lyman lines can be calculated and the ratio W/b obtained from the curve of growth. The equivalent width W in the Lyman lines is measured directly and the b value then determined. This analysis has been carried out using the HLδ, ϵ and η lines and the value obtained, $b = 6.5 \pm 0.5$ km s^{-1} is in excellent agreement with the value of 7.0 ± 0.5 km s^{-1} calculated above from the equivalent width ratios from the two stars, supporting the choice of a different b value for each star.

Using the b values deduced in the previous section and the measured equivalent widths shown in table 1, column densities of the observed interstellar ions have been calculated. The results are shown in table 2, which for completeness, also includes column densities of Na, Mg, Ca and

TABLE 2. INTERSTELLAR COLUMN DENSITIES

ion	γ^2 Vel lg (NL/m^{-2})	ζ Pup lg (NL/m^{-2})
H I	23.47–23.78	23.76–23.89
H II	24.32	24.32
total H	24.38–24.43	24.43–24.46
C II ($\mathcal{J} = 3/2$)	17.83–18.13	17.80–18.27
C II ($\mathcal{J} = 1/2$)	18.18–18.49	18.10–18.57
total C	18.34–18.65	18.28–18.75
N I	18.25–18.80	18.80–19.00
N II ($\mathcal{J} = 2$)	17.67–17.82	17.95–18.12
N II ($\mathcal{J} = 1$)	17.90–18.12	18.10–18.36
N II ($\mathcal{J} = 0$)	17.95–18.20	17.94–18.11
total N	18.59–18.99	18.97–19.17
O I	19.80–20.35	19.50–19.85
Na I*	15.76–15.96	15.80–16.00
Mg I*	16.24–16.44	16.37–16.57
Mg II*	18.40–18.80	18.90–19.06
total Mg	18.40–18.80	18.90–19.06
Al II	16.85–17.35	17.40–17.75
Al III	17.05–17.25	16.90–17.20
total Al	17.26–17.60	17.52–17.86
Si I	16.30–17.30	15.70–16.70
Si II	18.20–18.65	18.40–18.80
Si III	16.60–19.15	18.45–18.65
total Si	18.75–19.27	18.73–19.03
S II	19.10–19.40	19.25–19.40
S III	16.60–17.00	16.70–17.20
total S	19.10–19.40	19.25–19.40
Ar I	17.60–18.20	18.15–18.75
Ca II*	15.66–15.86	15.90–16.10
Fe II*	17.80–18.00	17.80–17.90

* Column densities for Na, Mg, Ca and Fe derived from published optical and u.v. data (see p. 360).

PHILOSOPHICAL TRANSACTIONS OF THE ROYAL SOCIETY A MATHEMATICAL, PHYSICAL & ENGINEERING SCIENCES

Fe, derived from optical observations of γ^2 Vel (Wallerstein & Silk 1971) and ζ Pup (Baschek & Scholz 1971*b*) and from ultraviolet observations of γ^2 Vel (Grewing, Lamers, Walmsley & Wulf-Mathies 1973) and ζ Pup (de Boer & Pottasch 1973). The range of ions observed is consistent with the line of sight to γ^2 Vel and ζ Pup traversing a large H II region. In an H I region, no significant amounts of Al III, Si III or S III would be expected since they are not produced by photons with wavelengths longward of the Lyman limit ($\lambda > 91.2$ nm). This is consistent with the model of the Gum Nebula proposed by Brandt *et al.* (1971), who suggested that about 350 pc of the total line of sight to ζ Pup was through the Gum H II region.

The absence of C I and weakness of Si I suggests that the line of sight is predominantly through a low density intercloud medium. The photoionization rate of C I to C II and Si I to Si II is only weakly dependent on the density since an interstellar cloud is largely transparent in the wavelength range 91–152 nm producing photoionization of C I or Si I. Recombination occurs rapidly at the higher gas densities within a typical cloud, but produces only a very small amount of neutral carbon and silicon in the low density intercloud medium.

Al III, Si III and S III represent the highest ionization stages observed, while C IV, N V, O VI, Si IV and S IV are below the limit of detectability in the present spectra. This would suggest that the ionization balance is determined mainly by u.v. photons and the diffuse X-ray background (Weisheit 1973).

Interstellar abundances

The determination of chemical abundances relative to hydrogen is complicated because the column density of interstellar H II is not directly measurable. In compiling table 2 we have used the dispersion measure to the Vela pulsar PSR 0833-45 (Ables, Komesaroff & Hamilton 1970) which determines the column density of electrons to the pulsar. This provides a measure of the H II density since in a predominantly H II region the electron density will be nearly equal to the H II density. The pulsar is within a few degrees of γ^2 Vel and ζ Pup, and it is usually assumed (e.g. by Brandt *et al.* 1971) to be located close to γ^2 Vel and ζ Pup.

Accordingly, the abundances have been calculated for two values of the interstellar hydrogen density, one for the 'total' hydrogen density (H I from the present data plus H II from the pulsar dispersion measure) and one for the H I density only. The results are shown in figure 3 as $\lg(N_X/N_H) - \lg(N_X/N_H)_\odot$, the logarithmic abundance relative to hydrogen in the line of sight, relative to the corresponding solar abundance taken from Allen (1973). The calculations are based on the 'total' hydrogen density (H I + H II) and the horizontal broken line shows the alternative reference level if only the interstellar H I is included. Some vertical bars in figure 3 have upward-pointing arrows to indicate that the measured abundance would be increased if it were possible to include other ionization states that are expected to be abundant in the interstellar medium, but which are not observable because their resonance absorption lines are at inaccessible wavelengths. The true abundances of these elements will be greater than indicated in figure 3 by an amount which depends on the ionization balance of the gas. In the case of nitrogen an upper limit to the abundance is indicated, which assumes that the Si II, N III blend at $\lambda = 98.98$ nm is due entirely to N III. All of the elements observed in the interstellar medium are found to be under-abundant relative to hydrogen, but the observed abundances of Al, Si, S and Ar relative to N are close to their solar values. Since there is very little reddening of stars in the region of the Gum Nebula, it is not possible to explain this depletion of heavier elements by condensation on grains.

PHILOSOPHICAL TRANSACTIONS OF THE ROYAL SOCIETY A MATHEMATICAL, PHYSICAL & ENGINEERING SCIENCES

Of the interstellar ions observed in the present spectra, C II, N II, N III, O I and Si II have more than one level in the ground term. Absorption lines from the excited fine structure levels are observed in C II and N II but not in N III, O I or Si II. The non-appearance of absorption lines from excited fine structure levels in O I and N III can be explained by the relatively high decay probability of the excited levels, requiring a very high gas density to produce an appreciable population in these levels. In N II and C II the radiative decay probability is much smaller and, according to the calculations of Bahcall & Wolf (1968), a neutral gas density of $N_{\mathrm{H}} \approx 10^{10}$ m^{-3} would be required to produce the observed population ratios in C II, N II, O I and Si II.

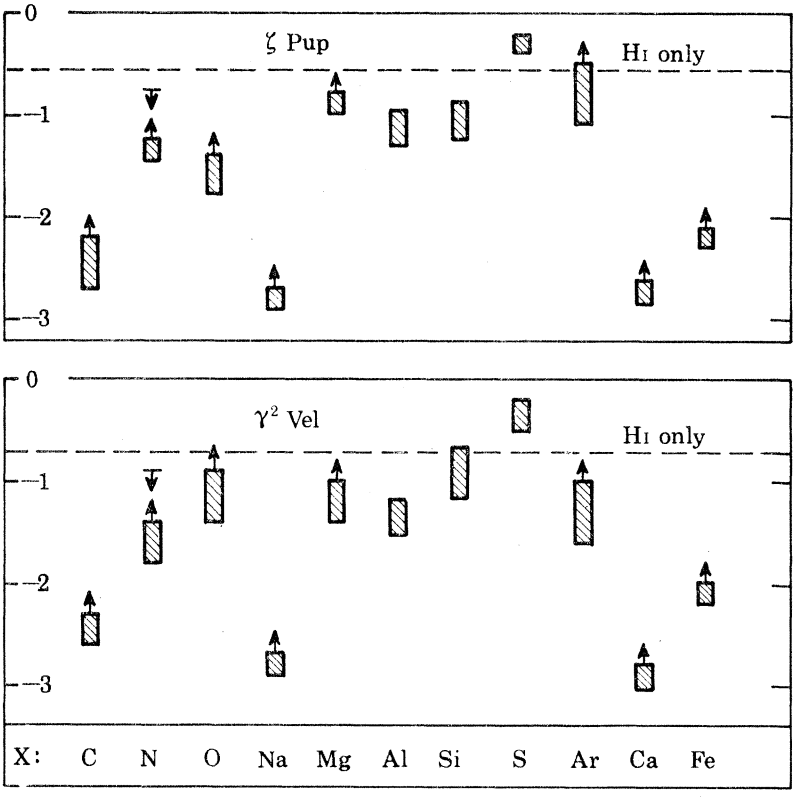

FIGURE 3. Relative interstellar abundances expressed as $\lg (N_{\mathrm{X}}/N_{\mathrm{H}}) - \lg (N_{\mathrm{X}}/N_{\mathrm{H}})_{\odot}$ measured for γ^2 Velorum and ζ Puppis. The broken horizontal line is an alternative zero level relating the abundances to H I only, instead of H I + H II.

A neutral gas density of 10^{10} m^{-3} is rather large for a region of interstellar space with no appreciable reddening and no obvious interstellar clouds in the visible absorption spectrum (Wallerstein & Silk 1971). If the excitation of the fine structure levels were by collisions with electrons rather than with neutral atoms then an electron density $n_{\mathrm{e}} \approx 10^8$ m^{-3} is required. However, in this case thermal equilibrium will exist only if the gas is predominantly neutral and a total gas density of $\approx 10^{10}$ m^{-3} is again required. This relatively high density need exist only in a few small localized regions in the line of sight in order to give a total column density consistent with the observed value.

PHILOSOPHICAL TRANSACTIONS OF THE ROYAL SOCIETY A MATHEMATICAL, PHYSICAL & ENGINEERING SCIENCES

The ζ Puppis spectrum

The optical spectrum of ζ Pup has recently been studied by Baschek & Scholz (1971*b*) who classified the star as O5f and by Heap (1972), who gave the classification O4f. The Of spectrum is well developed in that N III (λ = 464.0 nm) and He II (λ = 468.6 nm) are strongly in emission with a width indicative of a Doppler velocity of about 1000 km s^{-1}. Previous rocket observations of ζ Pup (Carruthers 1968; Morton *et al.* 1969; Stecher 1970; Smith 1970) have shown strong P Cygni profiles of several ultraviolet resonance lines indicative of a substantial mass loss rate. The present observations of ζ Pup give improved spectral resolution and cover a wider wavelength range than was obtained in the earlier observations. Within the wavelength range 100 to 230 nm covered in the present spectra O VI (λ = 103 nm), N V (λ = 124 nm), C IV (λ = 155 nm), He II (λ = 164 nm) and N IV (λ = 172 nm) are present in emission, and O VI (λ = 103 nm), S IV (λ = 106, 107 nm), C III (λ = 118 nm), N V (λ = 124 nm), Si IV (λ = 139 nm, 140 nm), C IV (λ = 155 nm) and N IV (λ = 172 nm) occur as violet-shifted absorption lines.

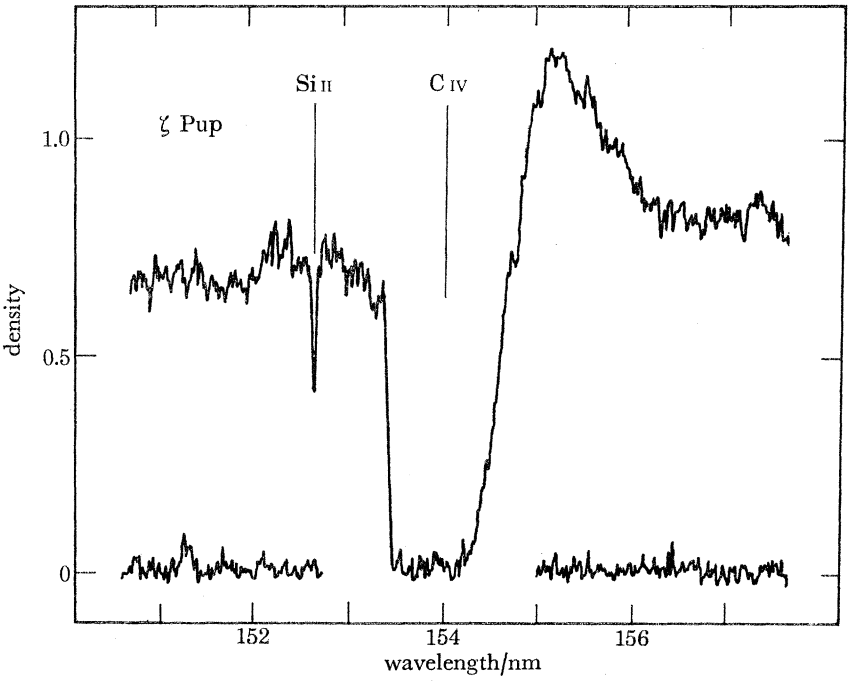

Figure 4. Densitometer tracing of the ζ Pup spectrum in the wavelength range 148–157 nm showing an interstellar line of Si II (λ = 152.6 nm) and the P Cygni profile of C IV (λ = 154.8 nm, λ = 155.1 nm).

There is a clear difference in the character of the absorption profile between the lines which have emission features and the pure absorption lines. The resonance lines which are in emission, e.g. C IV (λ = 155 nm), see figure 4, have an associated absorption which extends from essentially zero velocity to a well defined maximum velocity. Lines such as N IV (λ = 172 nm) which originate from excited levels have a smaller optical depth and do not show such a well defined maximum velocity. On the other hand the lines such as Si IV (λ = 140 nm) which occur only in absorption show well defined maximum and non-zero minimum velocities, between which strong absorption occurs. This suggests a pronounced stratification in the Of

atmosphere with each ionization stage existing within a well defined range of velocities. The lines which also have emission components presumably have larger optical depths than the other lines, the P Cygni profiles being formed by radiative transfer in an optically thick, radially expanding envelope. The measured expansion velocities are set out in table 3 below.

TABLE 3. MEASURED EXPANSION VELOCITIES FROM P CYGNI LINES

		γ^2 Vel V/km s^{-1}		ζ Pup V/km s^{-1}	
ion	λ/nm	min	max	min	max
C II	133.5	500	1500	—	—
C III	117.5	150	1730	1230	2040
	229.6	260	1580		
C IV	155.0	—	2320	—	2750
N IV	171.8	—	—	—	1900
N V	124.0	—	—	—	3200
Si III	120.6	570	1475	—	—
Si IV	139.4	390	1840	1000	2570
	140.2	420	1750	870	2570
S IV	106.3	450	1500	1300	2100
	107.3	450	1500	1500	2400

The largest velocity, 3200 km s^{-1} is observed in the P Cygni profile of N V (λ = 124 nm), suggesting that the velocity is positively correlated with ionization potential, or with electron temperature. Figure 5 shows the dependence of the range in observed velocities for each ion on the ionization potential of the next lower stage of ionization. There is evidence of a positive

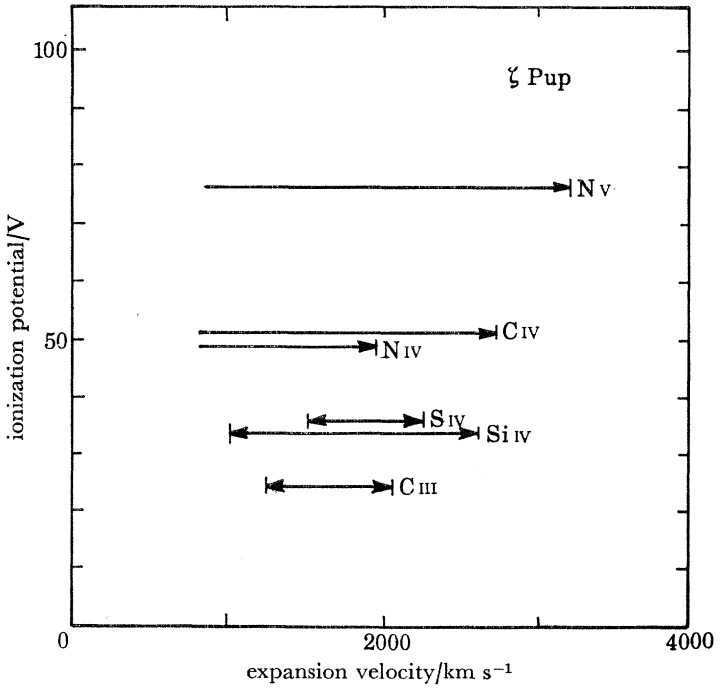

FIGURE 5. Measured expansion velocities corresponding to maximum and minimum wavelength shifts for absorption lines in the ζ Pup spectrum showing the ionization potential of the preceding stage for each ion.

correlation between the measured velocities and the ionization potentials, which would indicate an increase in velocity with temperature. This is in contrast to optical observations of Wolf-Rayet stars where the width of emission lines decreases with increasing temperature (e.g. Kuhi 1973).

It is possible to associate a definite temperature with each ionization stage by using the ionization balance calculations of Jordan (1969). These calculations are for collisional ionization followed by radiative recombination. Because of the neglect of photoionization the resulting values will not be strictly appropriate for the atmosphere of a hot star, nevertheless, the calculations serve to indicate an 'equivalent ionization temperature' which is a reflection of both the electron temperature and the strength of the stellar radiation field. Using the data in figure 5, we obtain figure 6 by calculating the range of electron temperature over which $> 1\,\%$ of the element will be in a particular ionization stage. The minimum temperature is then assigned to the minimum measured expansion velocity and the maximum temperature to the maximum velocity. The resulting data points shown in figure 6 give support to the suggested positive correlation of expansion velocity and temperature.

A more detailed analysis of the line profiles is continuing in an attempt to understand the structure of the extended Of atmosphere.

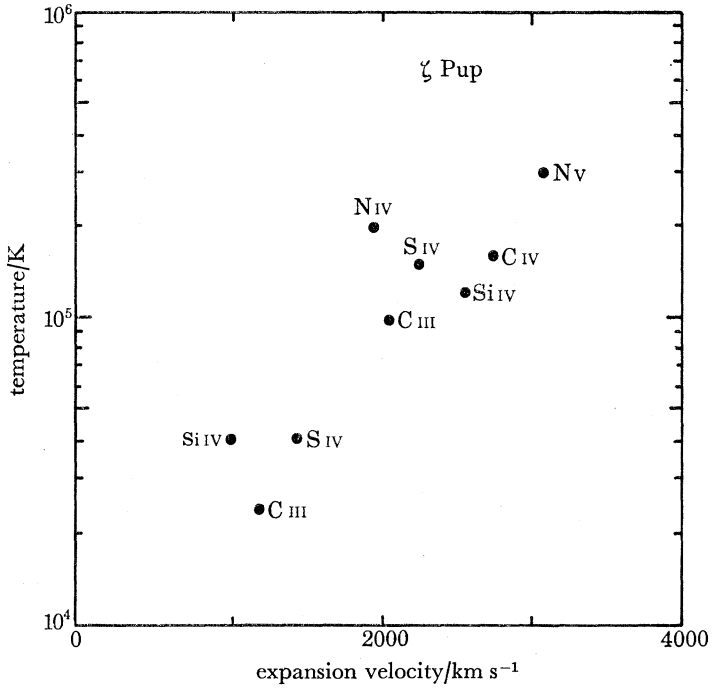

FIGURE 6. Equivalent ionization temperature limits for producing the observed ions in the ζ Pup spectrum plotted against minimum and maximum expansion velocity values.

THE γ^2 VELORUM SPECTRUM

The double star γ Vel has a B1 IV component (γ^1 Vel) separated by 42″ from the brighter ($\Delta m_v \approx 2.4$) component γ^2 Vel. The present observations are attributed to the two components of the spectroscopic binary system γ^2 Vel (WC8 + O8, $m_v = 1.8$). Baschek & Scholz (1971*a*) and Conti & Smith (1972) have described the visible composite spectrum of γ^2 Vel and both

studies conclude that the O8 component is brighter than the Wolf–Rayet component ($\Delta m_v \approx 1.5$) in this spectral region. In order to resolve the contributions of the two stars in the present ultraviolet composite spectrum it is useful to compare the γ^2 Vel spectrum with that of ζ Pup, which is classified as spectral type O5f (Baschek & Scholz 1970*b*) and might be expected to have some similarities with the O8 component of the γ^2 Vel system. Significant differences in the spectra of γ^2 Vel and ζ Pup can than be attributed to the presence of the Wolf–Rayet component of γ^2 Vel.

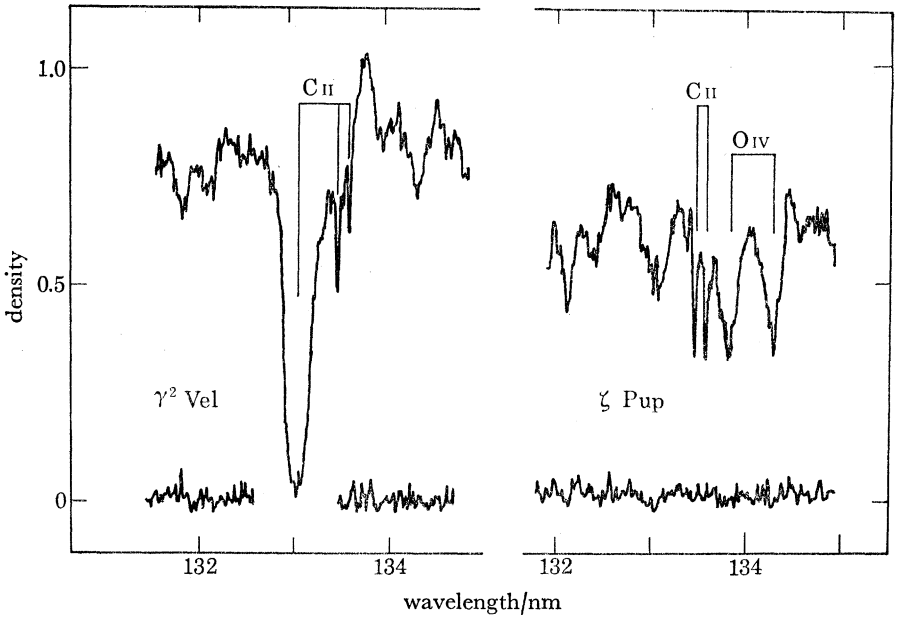

FIGURE 7. Densitometer tracings of the wavelength range 132–134 nm for ζ Pup and γ^2 Vel showing the interstellar absorption lines of C II (λ = 133.5, 133.6 nm) and the violet-shifted C II absorption feature in γ^2 Vel.

Figure 7 shows densitometer tracings of the two spectra in the wavelength region 132–134 nm. The interstellar absorption lines of C II (λ = 133.4, 133.6 nm) are prominent in both spectra but in γ^2 Vel they are accompanied by a broad deep absorption line on the shorter wavelength side. This feature reduces the stellar continuum almost to the clear film level at its centre in the γ^2 Vel spectrum but is very much weaker in ζ Pup. Similar violet-shifted absorption lines are observed in γ^2 Vel in several other spectral lines, including C II (λ = 103.6, 103.7 nm), C III (λ = 117.5, 190.9, 229.7 nm), Si III (λ = 120.6 nm), and S IV (λ = 106.3, 107.3 nm). As these features are generally much more prominent in γ^2 Vel than in ζ Pup it seems probable that they are associated with the extended atmosphere of the Wolf–Rayet system.

The interpretation of these features is not simple. If the violet-shifted absorption lines of C II at λ = 103.7 and 133.5 nm, which reduce the composite stellar continuum essentially to zero, are formed within the WR envelope then this implies that the O8 star is relatively weak at the wavelengths of the displaced C II lines. Since these lines are not expected to be strong or displaced in a normal O8 star, the stellar continuum level must be very low. However, this conclusion seems to be inconsistent with the accepted relative magnitudes of the two components of γ^2 Vel as estimated from the visible spectrum observations.

The ultraviolet spectrum could be explained if we assume that the expanding region of C II absorption in the WR star obscures the line of sight to the O8 component. At the time of

the observations, the WR star was near to the line of sight to the more distant O star, but an eclipse of this star by the WR envelope seems to be excluded if we adopt the orbital period of 78.5 d estimated by Ganesh & Bappu (1967) and the measurement by Hanbury Brown, Davis, Herbison-Evans & Allen (1970) of the diameter of the WR emission line envelope. A more probable explanation is that the C II absorption occurs in an expanding region, significantly more extended than the WR line emitting envelope. A tentative model for the γ^2 Vel binary system at the time of the present observations is shown in figure 8. The emission line envelope of the WC8 component is known to fill the Roche lobe around this star (Hanbury Brown *et al.* 1970) and produces a spectrum characterized by broad emission features, predominantly due to high level transitions in C III and C IV. We suggest that there is a significant flow of relatively cool gas which passes out of the Roche lobe and forms an expanding atmosphere around both the WR and O components of the binary system. At a temperature of about 2×10^4 K this atmosphere provides sufficient optical depth in the resonance lines of C II to produce the observed violet-shifted absorption lines at 103.6 and 113.4 nm.

A further problem is concerned with the absorption component in the P Cygni profile of the C III line at 190.9 nm, a densitometer tracing of which is shown in figure 9. Because this line is an intersystem transition ($2s\ ^1S_0 - 2p^3P_1$) with a low transition probability ($A \approx 190\ s^{-1}$),

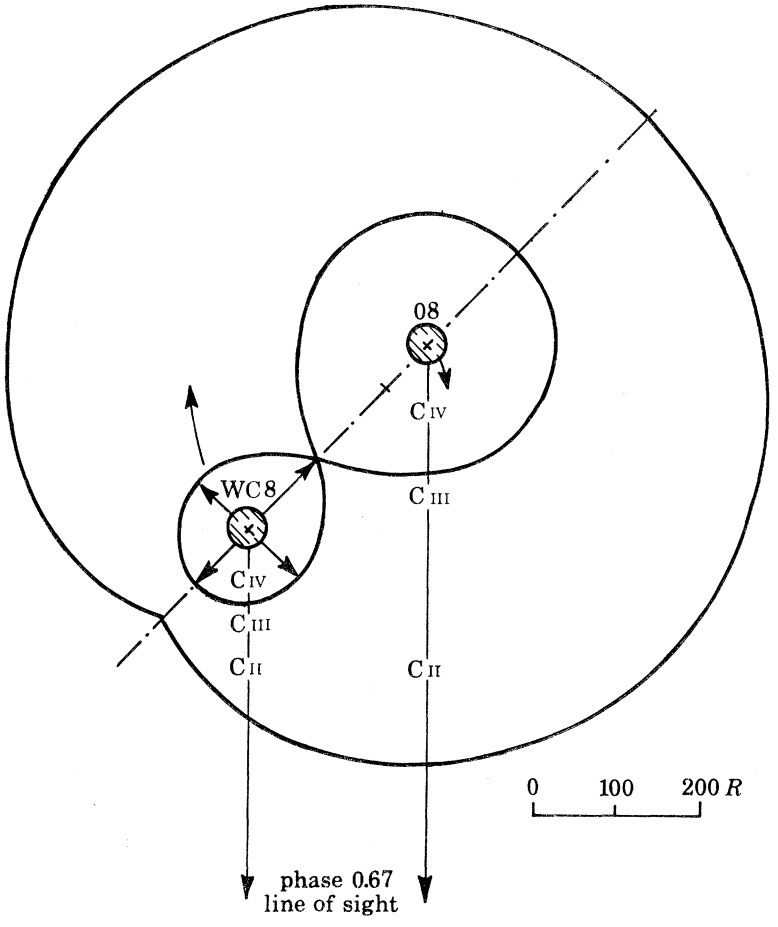

FIGURE 8. Suggested model of the γ^2 Vel binary system at the time of the present ultraviolet spectrum observations indicating where the ions forming the observed adsorption spectrum might be located. The scale is based on the measurements of Hanbury Brown *et al.* (1970) adjusted for the adopted distance of 450 pc.

the strength of the absorption line implies a very high column density in C III. This line is not observed in ζ Pup and is probably not present in the O8 component of γ^2 Vel. If we assume that the C III line is formed in the WR envelope, then the WR continuum flux at 190.9 nm must be slightly greater than the continuum flux of the O star because the line removes a substantial fraction of the continuum. However, if the absorption occurs in an extended atmosphere which encloses both stars, then the O star continuum flux could be relatively greater and thus consistent with the observed visible spectrum. The C III line at $\lambda = 229.7$ nm which has a deep P Cygni absorption component similar to the $\lambda = 190.9$ nm line could also be explained in this way.

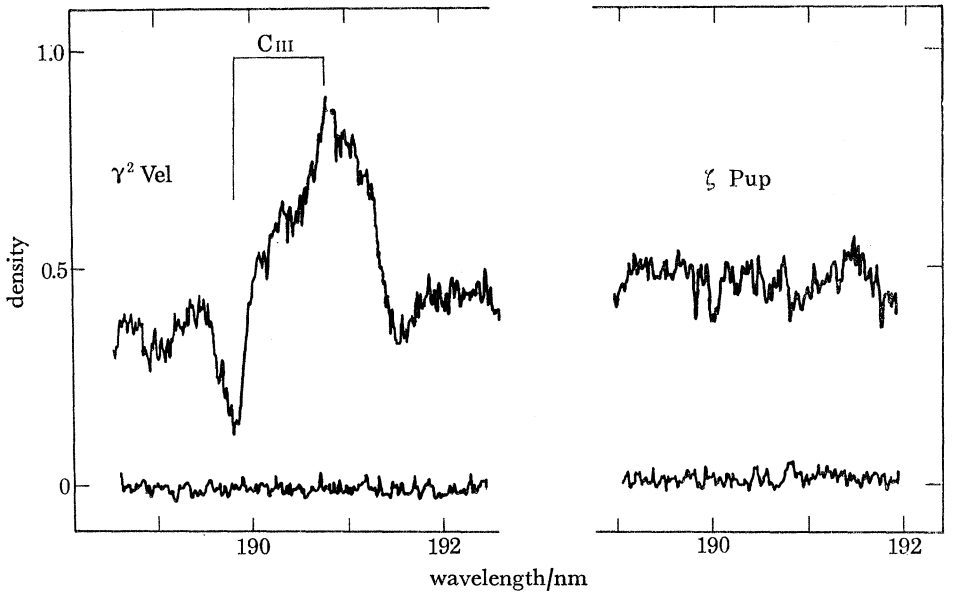

FIGURE 9. Densitometer tracing of the wavelength range 189–193 nm for ζ Pup and γ^2 Vel showing the C III intersystem line at λ 190.9 nm in γ^2 Vel.

The resonance multiplet of C IV (λ 154.8, 155.0 nm) in γ^2 Vel has a line profile generally similar to that observed in ζ Pup (see figure 4) with a broad violet-shifted absorption line which reduces the continuum flux to clear-film level. However, the γ^2 Vel absorption line has a smaller violet-shift than in ζ Pup and it does not show the unshifted emission component seen in ζ Pup. The total removal of continuum flux in the C IV absorption line in γ^2 Vel is most probably caused by the components in the binary system having similar mass-loss velocities which produce overlapping P Cygni profiles. An alternative explanation is that the continuum flux of one component is very weak in the wavelength range of the C IV absorption line or, as discussed above, that the absorption line is formed in a very extensive expanding atmosphere. However, it seems unlikely that C IV would be an abundant ion in such a region.

Whatever model is adopted for the γ^2 Vel atmosphere, it is appropriate to measure the dependence of expansion velocity on temperature using the procedure described for ζ Pup in the previous section. The variation of velocity with ionization potential is shown in figure 10 and the corresponding temperature dependence is given in figure 11. The data in figure 10 suggest that a narrower range of velocities is present in γ^2 Vel than in ζ Pup and there is some indication of a limiting velocity of about 2000 km s^{-1}. The positive correlation of velocity with temperature observed for ζ Pup is also found in γ^2 Vel (see figure 11). This result contrasts

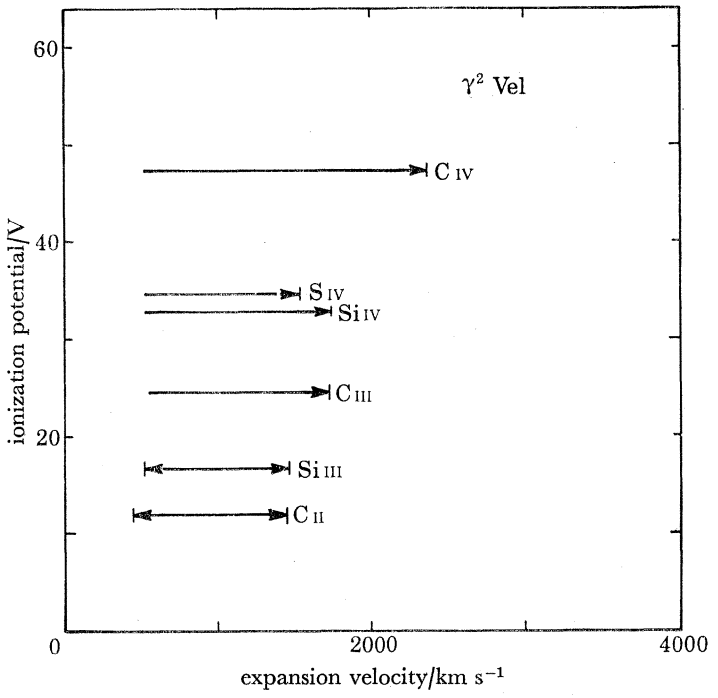

FIGURE 10. Measured expansion velocities corresponding to maximum and minimum wavelength shifts for absorption lines in the γ^2 Vel spectrum showing the ionization potential of the preceding stage for each ion.

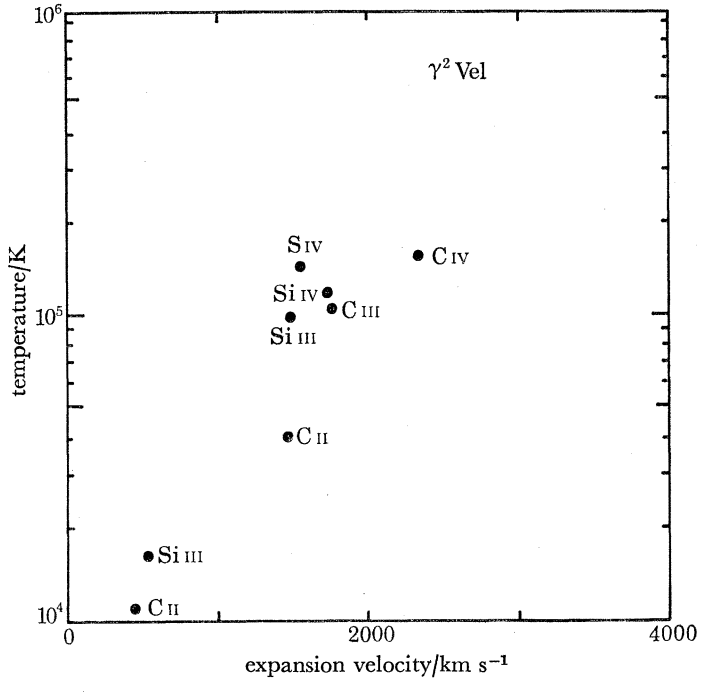

FIGURE 11. Equivalent ionization temperature limits for producing the ions in the γ^2 Vel spectrum plotted against minimum and maximum expansion velocity values.

with the negative correlation observed for the velocities deduced from Wolf–Rayet emission line widths at longer wavelengths (Kuhi 1973). However, the line width measurements probably relate to the velocity dispersion in the line emitting region while the present observations of wavelength-shifted resonance lines relate to an extended atmosphere surrounding the WR star. The data shown in figure 11 are best explained by assuming that the outward velocity and the temperature of the WR atmosphere both decrease with increasing radial distance in this outer region.

The new observations will permit a more detailed study of the conditions existing in the γ^2 Vel binary system.

The observations described in this paper were obtained by the collaborative efforts of many individuals. Professor R. Wilson, Dr A. Boksenberg, Dr F. Macchetto and Mr D. B. Shenton made important contributions to the success of the rocket experiment. The instrumentation was prepared at Culham with the help of Mr C. Lewis, Mr H. J. B. Paxton and Mr D. C. Tredgett. Payload integration was carried out by the British Aircraft Corporation at Filton and the rocket vehicle preparation was completed by B.A.C. (Australia) and Marconi Space and Defence Systems at Woomera, South Australia.

References (Burton *et al.*)

Ables, J. G., Komesaroff, M. M. & Hamilton, P. A. 1970 *Astrophys. Lett.* **6**, 147–150.
Allen, C. W. 1973 *Astrophysical quantities*, 3rd ed., pp. 30–33. London: Athlone Press.
Bahcall, J. N. & Wolf, R. A. 1968 *Astrophys. J.* **152**, 701–729.
Baschek, B. & Scholz, M. 1971*a* *Astron. Astrophys.* **11**, 83–88.
Baschek, B. & Scholz, M. 1971*b* *Astron. Astrophys.* **15**, 285–291.
Boer, K. S. de & Pottasch, S. R. 1973 *Astron. Astrophys.* **28**, 155–158.
Bok, B. 1971 *The Gum Nebula and related problems*, 148–149. NASA Special Publication SP-332.
Brandt, J. C., Stecher, T. P., Crawford, D. L. & Maran, S. P. 1971 *Astrophys. J.* **163**, L99–L104.
Burton, W. M., Evans, R. G., Griffin, W. G., Lewis, C., Paxton, H. J. B., Shenton, D. B., Macchetto, F., Boksenberg, A. & Wilson, R. 1973 *Nature* (*Phys. Sci.*) **246**, 37–40.
Burton, W. M., Evans, R. G. & Griffin, W. G. 1974 *Mon. Not. R. astr. Soc.* **169**, 307–321.
Carruthers, G. R. 1968 *Astrophys. J.* **151**, 269–284.
Conti, P. S. & Smith, L. F. 1972 *Astrophys. J.* **172**, 623–630.
Ganesh, K. S. & Bappu, M. K. V. 1967 *Bull. Kodaikánal Obs.* A **183**, 177–191.
Grewing, M., Lamers, H. J., Walmsley, C. M. & Wulf-Mathies, C. 1973 *Astron. Astrophys.* **27**, 115–118.
Hanbury Brown, R., Davis, J., Herbison-Evans, D. & Allen, L. R. 1970 *Mon. Not. R. astr. Soc.* **148**, 103–117.
Heap, S. 1972 *Astrophys. Lett.* **10**, 49–53.
Jordan, C. 1969 *Mon. Not. R. astr. Soc.* **142**, 501–521.
Kuhi, L. V. 1973 *Astrophys. J.* **180**, 783–789.
Macchetto, F. & Panagia, N. 1973 *Astron. Astrophys.* **28**, 313–314.
Morton, D. C., Jenkins, E. B. & Brooks, N. H. 1969 *Astrophys. J.* **155**, 875–885.
Smith, A. M. 1970 *Astrophys. J.* **160**, 595–608.
Stecher, T. P. 1970 *Astrophys. J.* **159**, 543–550.
Wallerstein, G. & Silk, J. 1971 *Astrophys. J.* **170**, 289–296.
Weisheit, J. C. 1973 *Astrophys. J.* **185**, 877–886.

PHILOSOPHICAL TRANSACTIONS OF THE ROYAL SOCIETY A MATHEMATICAL, PHYSICAL & ENGINEERING SCIENCES